Research Article

Cancer Prevention Research

5-Deoxykaempferol Plays a Potential Therapeutic Role by Targeting Multiple Signaling Pathways in Skin Cancer

Kyung Mi Lee[1,2,3], Ki Won Lee[1,3], Sanguine Byun[2,3], Sung Keun Jung[2,3], Sang Kwon Seo[2], Yong-Seok Heo[4], Ann M. Bode[1], Hyong Joo Lee[2], and Zigang Dong[1]

Abstract

Nontoxic small molecules with multitargeting effects are believed to have potential in cancer prevention. Dietary phytochemicals were shown to exhibit cancer-preventive effects attributed to their antioxidant capacities. In this report, we show that the natural compound 5-deoxykaempferol (5-DK) exerts a chemopreventive effect on UVB-induced skin carcinogenesis by targeting multiple signaling molecules. 5-DK suppressed the UVB-induced expression of cyclooxygenase-2 (COX-2) and vascular endothelial growth factor in mouse skin epidermal JB6 P+ cells. Moreover, 5-DK inhibited phosphorylation of MKK3/6, MKK4, and Akt, but had no effect on phosphorylation of Src, extracellular signal–regulated kinases, or ribosomal S6 kinase (RSK). However, 5-DK affected multiple targets by reducing Src, phosphoinositide 3-kinase (PI3K), and RSK2 activities. In particular, pull-down assays revealed that 5-DK specifically bound to and competed with ATP for binding with Src, PI3K, and RSK2. Exposure to 5-DK significantly suppressed UVB-induced tumorigenesis in mouse skin in a dose-dependent manner, and it inhibited the UVB-induced expression of COX-2, proliferating cell nuclear antigen, vascular endothelial growth factor, and matrix metalloproteinase-9. Our data suggest that 5-DK docks at the ATP-binding site of Src, PI3K, and RSK2. For RSK2, the ATP-binding site is located between the N- and C-lobes of the kinase domain. Taken together, our results indicate that 5-DK holds promise for the treatment of UVB-induced skin cancer by targeting Src, PI3K, and RSK2 signaling. *Cancer Prev Res; 3(4); 454–65. ©2010 AACR.*

Introduction

Skin cancer is one of the most commonly diagnosed cancers, with an estimated 1 million new cases reported each year in the United States. Repeated and excessive exposure to UV irradiation eventually causes skin cancer. In particular, UVB is a key contributor serving as complete carcinogen, acting as a tumor initiator and promoter in humans (1). UVB irradiation triggers inflammation and angiogenesis, which promotes the development of malignancies (2, 3). A high level of cyclooxygenase-2 (COX-2), which is a major inducible enzyme in the biosynthesis of prostaglandins, has been shown to be a primary mediator of inflammation and carcinogenesis (4). In addition, vascular endothelial growth factor (VEGF) plays a crucial role in vascularization in the development of inflammatory skin diseases, including skin cancer (5).

In photocarcinogenesis, the activation of various signaling molecules, including numerous nonreceptor tyrosine and serine/threonine kinases, plays an important role in the clonal expansion of UVB-initiated cells into visible skin tumors (6). Src, which is a nonreceptor tyrosine protein kinase, is overexpressed and highly activated in various cancers; moreover, increased Src activity has oncogenic potential in tumor cell development (7, 8). The Src-family tyrosine kinases are involved in signal transduction pathways that regulate such physiologic processes as proliferation, survival, metastasis, and angiogenesis (9, 10). Src is a critical component of the signaling pathways that control tumor development, and thus, it is also an appealing target for cancer prevention. In addition, UV radiation induces the activation of protein kinase cascades, including the mitogen-activated protein kinases (MAPK) and phosphoinositide 3-kinase (PI3K)/Akt cascades. The MAPKs and PI3K/Akt signaling pathways play important regulatory roles in a variety of cellular functions, including COX-2 and VEGF expression (11, 12). Based on these data, the idea of targeting multiple signaling pathways has emerged as a promising approach for the innovative and effective medical treatment of skin cancer.

Flavonoids are naturally occurring compounds that are believed to exhibit preventive effects in various diseases, including cancer. For many years, the anticancer activities

Authors' Affiliations: [1]The Hormel Institute, University of Minnesota, Austin, Minnesota; [2]Major in Biomodulation, Department of Agricultural Biotechnology, Seoul National University; and [3]Bio/Molecular Informatics Center, Department of Bioscience and Biotechnology and [4]Department of Chemistry, Konkuk University, Seoul, Republic of Korea

Note: K.M. Lee, K.W. Lee, and S. Byun contributed equally to this work.

Corresponding Authors: Hyong Joo Lee, Major in Biomodulation, Department of Agricultural Biotechnology, Seoul National University, Seoul 151-742, Republic of Korea. Fax: 82-2-873-5095; E-mail: leehyjo@snu.ac.kr or Zigang Dong, The Hormel Institute, University of Minnesota, 801 16th Avenue Northeast, Austin, MN 55912. Phone: 507-437-9600; Fax: 507-437-9606; E-mail: zgdong@hi.umn.edu.

doi: 10.1158/1940-6207.CAPR-09-0137

of flavonoids were attributed to their antioxidant activities. Thus, the determination of novel targets for the chemopreventive effects of flavonoids was largely ignored. Recently, some small-molecule inhibitors have proved to be effective in cancer prevention because they target multiple protein kinases (13, 14). The cancer chemopreventive effect of 5-deoxykaempferol (5-DK), which is a natural compound derived from *Anthyllis vulneraria* (15), is unknown. Herein, we report that 5-DK suppresses UVB-induced expression of COX-2 and VEGF through direct inhibition of Src, PI3K, and ribosomal S6 kinase-2 (RSK2) activities. Topical treatment with 5-DK also significantly repressed UVB-induced skin cancer in mice. Thus, 5-DK acts as an inhibitor of Src, PI3K, and RSK signaling and is expected to have beneficial effects in the prevention or treatment of skin cancer.

Materials and Methods

Materials

5-Deoxykampferol was purchased from Indofine Chemical Co. Eagle's MEM, gentamicin, and L-glutamine were obtained from Life Technologies, Inc. Fetal bovine serum (FBS) was purchased from Sigma-Aldrich. An ELISA kit for the measurement of VEGF was purchased from R&D Systems. The COX-2–specific antibody was purchased from Cayman, and the β-actin–specific antibody was purchased from Sigma-Aldrich. The antibodies used to detect phosphorylated p38 (Tyr180/Tyr182), total p38, phosphorylated c-jun NH_2-terminal kinase (JNK) (Thr183/Tyr185), total JNK, phosphorylated Akt, total Akt, phosphorylated MKK3/6, total MKK3, phosphorylated MKK4, total MKK4, phosphorylated p90RSK (Thr359/Ser363), total p90RSK, and phosphorylated Src (Y416) were purchased from Cell Signaling Biotechnology. Antibodies against total Src were obtained from Upstate Biotechnology. Antibodies against VEGF and proliferating cell nuclear antigen (PCNA) were obtained from Santa Cruz Biotechnology. CNBr-Sepharose 4B, glutathione-Sepharose 4B, [γ-^{32}P]ATP, and the chemiluminescence detection kit were purchased from Amersham Pharmacia Biotech, whereas the protein assay kit was obtained from Bio-Rad Laboratories.

Cell culture

JB6 P+ mouse epidermal cells were cultured in monolayers at 37°C under 5% CO_2 in 5% FBS-MEM that contained 2 mmol/L L-glutamine and 25 μg/mL gentamicin.

Animals

SKH-1 hairless mice (6 wk of age; mean body weight, 25 g) were purchased from the Seoul National University Institute of Laboratory Animal Resources (Seoul, Korea). The animals were stabilized for 1 wk before the study and had free access to food and water for the entire study. The animals were housed in climate-controlled quarters (24°C at 50% humidity) with a 12-h light/12-h dark cycle.

In vitro Western blotting

For our Western blot assay, 1.5×10^6 cells were cultured in a 10-cm dish for 48 h and then starved in 0.1% FBS-MEM for 24 h to eliminate the FBS activation of MAPKs. The cells were then treated with 5-DK (0, 10, 20, or 40 μmol/L) for 30 min and irradiated with 0.05 J/cm^2 UVB. The harvested cells were then disrupted with lysis buffer [10 mmol/L Tris (pH 7.5), 150 mmol/L NaCl, 5 mmol/L EDTA, 1% Triton X-100, 1 mmol/L DTT, 0.1 mmol/L phenylmethylsulfonyl fluoride (Calbiochem), 10% glycerol, and a protease inhibitor cocktail tablet] and the supernatant fractions were boiled for 5 min. The protein concentration was determined using a dye-binding protein assay kit (Bio-Rad Laboratories) as described in the manufacturer's manual. Lysates were then prepared, subjected to 10% SDS-PAGE (40 μg/well), and transferred onto polyvinylidene difluoride membranes (Amersham Pharmacia Biotech). After blotting, the membranes were incubated overnight at 4°C with the primary antibody. The bands were visualized using a chemiluminescence detection kit (Amersham Pharmacia Biotech) after hybridization with a horseradish peroxidase–conjugated secondary antibody. The relative amount of protein associated with each specific antibody was quantified using Scion Image (NIH).

Determination of VEGF production

JB6 P+ cells (5×10^5) were cultured in 96-well plates and incubated for 48 h. The cells were then pretreated with 5-DK (10, 20, or 40 μmol/L) for 30 min, irradiated with UVB (0.05 J/cm^2), and harvested 12 h later. The amount of VEGF in the culture medium was measured according to the manufacturer's instructions. The data were normalized by the protein concentration in each sample.

Src, RSK2, extracellular signal–regulated kinase-2, p38, and JNK1 assays

The kinase assays were done in accordance with the instructions provided by Upstate Biotechnology. The effects of 5-DK (0-40 μmol/L) were evaluated using reaction mixtures held at 30°C for 30 min. Each experiment was done three times.

PI3K assay

Active PI3K (100 ng) was incubated with 5-DK for 10 min at 30°C. The mixture was then incubated with 20 μL of 0.5 mg/mL phosphatidylinositol (Avanti Polar Lipids) for 5 min at room temperature, followed by incubation with reaction buffer [100 mmol/L HEPES (pH 7.6), 50 mmol/L $MgCl_2$, and 250 μmol/L ATP containing 10 μCi of [γ-^{32}P]ATP] for an additional 10 min at 30°C. The reaction was stopped by the addition of 15 μL of 4 N HCl and 130 μL of chloroform/methanol (1:1). After vortexing, 30 μL of the lower chloroform phase were spotted onto a 1% potassium oxalate–coated silica gel plate that had been previously activated for 1 h at 110°C. The resulting ^{32}P-labeled phosphatidylinositol-3-phosphate was separated by TLC, and the radiolabeled spots were visualized by autoradiography.

Mouse skin tumorigenesis analysis

The UVB irradiation source (Bio-Link Crosslinker, Vilber Lourmat) emitted at wavelengths of 254, 312, and 365 nm, with peak emission at 312 nm. SKH-1 mice were divided into four groups of 15 animals each: the control group, the UVB group, and two 5-DK–treated groups. The control mice were treated topically with 200 μL of acetone. In the UVB group, the mice were treated topically with 200 μL of acetone before treatment with 0.18 J/cm^2 UVB. The mice in the third and fourth groups were treated topically with 5-DK 1 h before irradiation with 0.18 J/cm^2 UVB. The frequency of irradiation was set at three times per week for 27 wk. The respective doses of 5-DK (8 or 20 nmol in 200 μL of acetone per mouse) and UVB (0.18 J/cm^2) were topically applied to the dorsal area. The incidence of skin tumors was recorded weekly. A tumor was defined as an outgrowth >1 mm in diameter that persisted for 2 wk or more. Tumor incidence, multiplicity, and volume were recorded each week until the end of the experiment at 27 wk.

Preparation of skin lysates

Mice treated topically on their backs with 5-DK (8 or 20 nmol in 200 μL of acetone) 1 h before UVB irradiation were sacrificed after the last round of UVB exposure. For protein isolation, the dorsal skin of each mouse was excised, the fat was removed on ice, and the skin was immediately pulverized in a mortar using liquid nitrogen. The pulverized skin was then homogenized on ice (IKA T10 basic homogenizer, Staufen) and the proteins were extracted using a 20% SDS solution that contained 1 mmol/L phenylmethylsulfonyl fluoride, 10 mmol/L iodoacetamide, 1 mmol/L leupeptin, 1 mmol/L antipain, 0.1 mmol/L sodium orthovanadate, and 5 mmol/L sodium fluoride. The lysates were centrifuged at 12,000 rpm for 20 min. Each supernatant fraction was collected and the protein concentration was determined using the Bio-Rad protein assay kit.

In vivo Western blotting

For Western blotting, skin lysates prepared from the epidermis and dermis were centrifuged at 12,000 rpm for 20 min and the protein content was determined using the Bio-Rad protein assay kit. A sample of each mouse skin extract (100 μg) was subjected to 10% SDS-PAGE and then transferred onto a polyvinylidene difluoride membrane (GE Healthcare). After blotting, the membrane was incubated overnight with the primary antibody at 4°C. The bands were visualized using a chemiluminescence detection kit (Amersham Pharmacia Biotech) after hybridization with a horseradish peroxidase–conjugated secondary antibody. The relative amount of protein associated with each antibody was quantified using Scion Image (NIH).

Gelatin zymography

To assess the gelatinolytic activity of matrix metalloproteinase (MMP)-9, gelatin zymography was conducted as follows. The protein content was determined using the Bio-Rad protein assay kit, and equal amounts of conditioned media were mixed with nonreducing sample buffer, incubated for 15 min at room temperature, and separated by 10% SDS-PAGE using gels that contained 1 mg/mL gelatin. After electrophoresis, the gels were washed twice with 2.5% Triton X-100 for 30 min each; rinsed three times for 30 min each with 50 mmol/L Tris-HCl buffer (pH 7.6) that contained 5 mmol/L $CaCl_2$, 0.02% Brij-35, and 0.2% sodium azide; and incubated overnight at 37°C. The gels were then stained with a 0.5% Coomassie brilliant blue R-250 solution that contained 10% acetic acid and 20% methanol for 30 min and destained with a 7.5% acetic acid solution that contained 10% methanol. Areas of gelatinase activity were detected as clear bands against the blue-stained gelatin background. Protein quantification was achieved by densitometric analysis of the protein bands (as scanned JPEG images) using the Image J software.

Immunohistochemical analysis

The expression profiles of COX-2, PCNA, and VEGF were analyzed in UVB-treated (0.18 J/cm^2) mouse skin treated or not treated with 5-DK (8 or 20 nmol/L in 200 μL of acetone). Sections (5 μm thick) of 10% neutral formalin solution–fixed, paraffin-embedded tissue were cut on silane-coated glass slides, deparaffinized three times with xylene, and then dehydrated through a graded alcohol series. The deparaffinized sections were boiled in 10 mmol/L citric acid buffer (pH 6.0) for antigen retrieval. To remove nonspecific staining, each section was treated with 3% hydrogen peroxide for 20 min and with 1% bovine serum albumin blocking solution for 2 h. For detection of the target protein, the slides were incubated with affinity-purified primary antibodies at 4°C overnight in 1% bovine serum albumin and then developed using the antirabbit or antimouse horseradish peroxidase EnVision System (Dako). The peroxidase binding sites were detected by staining with 3,3-diaminobenzidine tetrahydrochloride (Dako). Counterstaining was done with Mayer's hematoxylin.

Molecular modeling

The Insight II program (Accelrys, Inc.) was used for the docking and structural analyses with the crystal coordinates for Src (accession code 1YOJ), PI3K (1E8X), and RSK2 (2QN8) from the Protein Data Bank.[5]

Statistical analysis

The data are expressed as mean ± SD. The Student *t* test was used for single statistical comparisons, with $P < 0.05$ used as the criterion for statistical significance.

Results

5-DK suppresses UVB-induced expression of COX-2 and VEGF in JB6 P+ cells

We examined the effect of 5-DK on UVB-induced COX-2 expression in mouse epidermal JB6 P+ cells. 5-DK dose-dependently inhibited UVB-induced COX-2

[5] http://www.rcsb.org/pdb/

expression (Fig. 1B) and UVB-induced *cox-2* promoter activity (data not shown). Next, we examined whether 5-DK was capable of preventing UVB-induced VEGF secretion and found that 5-DK significantly attenuated UVB-induced expression of VEGF (Fig. 1C). Thus, 5-DK regulates UVB-induced COX-2 and VEGF expression in JB6 P+ cells.

5-DK inhibits UVB-induced phosphorylation of p38, JNK, and Akt but has no effect on phosphorylation of Src, extracellular signal–regulated kinase, or RSK in JB6 P+ cells

To determine the effect of 5-DK on UVB-induced signaling, JB6 P+ cells were treated with increasing concentrations of 5-DK (0, 10, 20, and 40 μmol/L) for 30 minutes and then exposed to UVB irradiation. The phosphorylation of p38, JNK, and Akt, but not of extracellular signal–regulated kinase (ERK; Fig. 1D, left), was inhibited by 5-DK. In addition, 5-DK blocked the phosphorylation of MKK3/6 and MKK4, which are specific upstream activators of p38 and JNK, whereas it had no effect on the UVB-induced phosphorylation of Src (Fig. 1D, right). Furthermore, 5-DK did not affect the UVB-induced phosphorylation of RSK, a downstream kinase of ERK (Fig. 1D, right). These results suggest that the inhibition of p38, JNK, and Akt signaling by 5-DK leads to decreased COX-2 and VEGF expression.

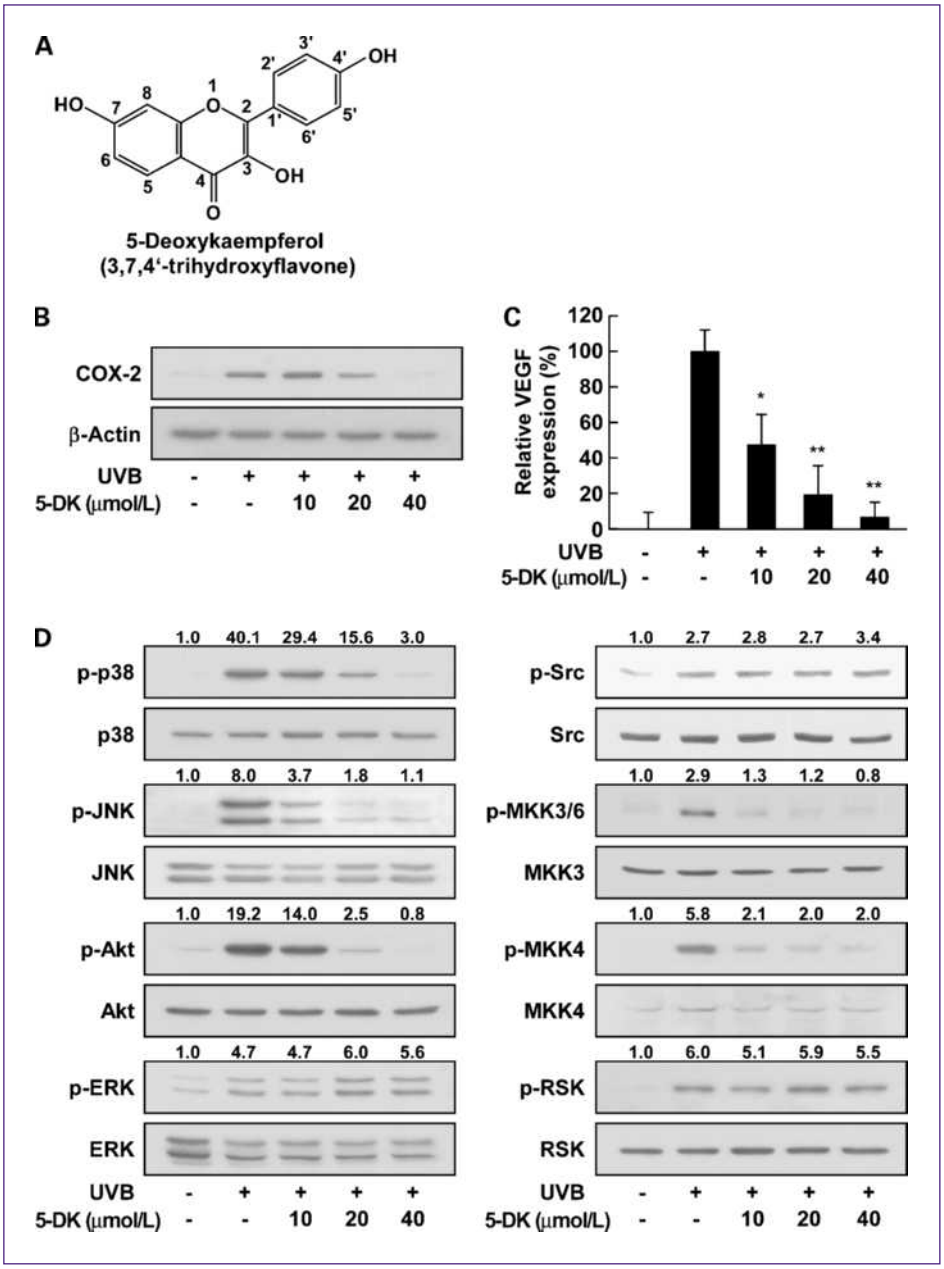

Fig. 1. Effects of 5-DK on UVB-induced COX-2 and VEGF expression and UVB-mediated signaling. A, chemical structure of 5-DK including the numbering scheme. B, 5-DK inhibits UVB-induced COX-2 expression in JB6 P+ cells. Cells were pretreated with 5-DK at the indicated concentrations (0, 10, 20, or 40 μmol/L) for 30 min, then stimulated with UVB (0.05 J/cm^2) and harvested 4 h later. COX-2 and β-actin expression were assessed by Western blot analysis as described in Materials and Methods, using antibodies against the respective proteins. C, 5-DK inhibits UVB-induced VEGF expression in JB6 P+ cells. Cells were treated with 5-DK at the indicated concentrations (0, 10, 20, or 40 μmol/L) for 30 min, then stimulated with UVB (0.05 J/cm^2) and harvested 12 h later. The conditioned medium was then collected and analyzed by ELISA for VEGF expression as described in Materials and Methods. *, $P < 0.05$; **, $P < 0.01$, significant decrease in VEGF expression in the 5-DK– and UVB-treated group compared with the group irradiated with UVB alone. D, 5-DK inhibits UVB-induced phosphorylation (p-) of p38, JNK, Akt, MKK3/6, and MKK4, but not of Src, ERK, or RSK2. Cells were treated with 5-DK at the indicated concentrations (0, 10, 20, or 40 μmol/L) for 30 min, then stimulated with UVB (0.05 J/cm^2) and harvested 15 or 30 min later. The levels of phosphorylated and total p38, JNK, Akt, ERK, Src, MKK3/6, MKK4, and RSK2 were determined by Western blotting as described in Materials and Methods, using antibodies against the corresponding phosphorylated and total proteins. Representative data of three independent experiments that gave similar results.

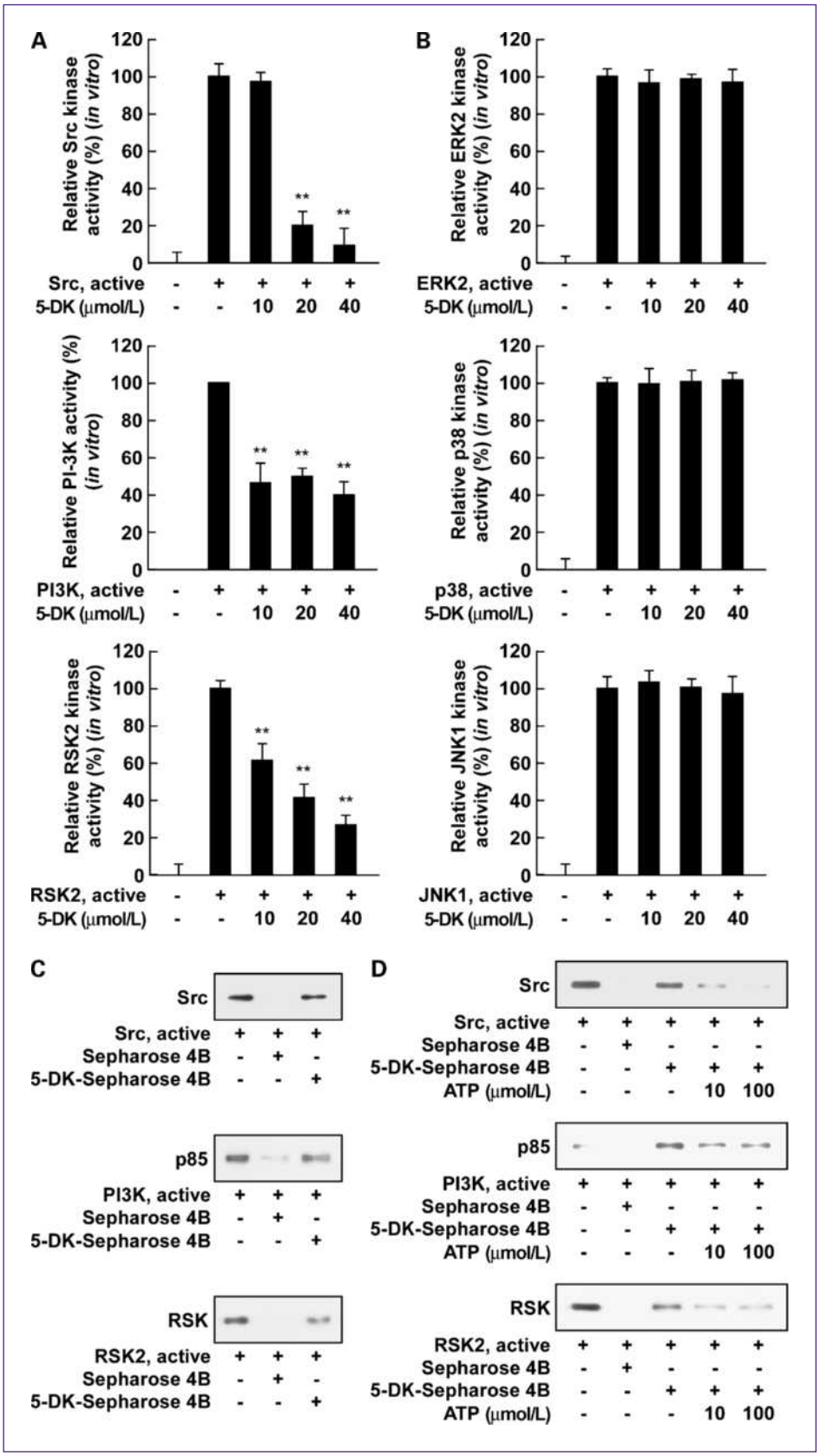

Fig. 2. Effects of 5-DK on Src, PI3K, RSK2, ERK2, p38, and JNK1 kinase and binding activities. A, 5-DK inhibits Src, PI3K, and RSK2 kinase activities. Src, PI3K, and RSK2 kinase assays were done as described in Materials and Methods. The effects of 5-DK on Src, PI3K, and RSK2 are expressed as percent inhibition relative to the level of activity in the untreated control. B, 5-DK has no effect on ERK2, p38, or JNK kinase activities. ERK2, p38, and JNK1 kinase assays were done as described in Materials and Methods. The effects of 5-DK on ERK2, p38, and JNK1 are expressed as percent inhibition relative to the level of activity in the untreated control. For A and B, the mean ^{32}P count was determined from three independent experiments (columns, mean; bars, SD). **, $P < 0.01$, significant decrease in activity for the group irradiated with UVB and treated with 5-DK versus the group exposed to UVB alone. C, 5-DK binds directly to Src, PI3K, or RSK2. The binding of 5-DK to Src, PI3K, or RSK2 was confirmed by immunoblotting using antibodies against Src, p85 (for PI3K), and RSK (for RSK2), respectively. Lane 1, Src, PI3K, or RSK2 as the input control; lane 2, negative control (Sepharose 4B was used to pull down Src, PI3K, or RSK2 as described in Materials and Methods); lane 3, Src, PI3K, and RSK2 were pulled down using 5-DK-Sepharose 4B affinity beads. D, 5-DK binds Src, PI3K, or RSK2 in an ATP-competitive manner. Active Src, PI3K, or RSK2 (2 μg) was incubated with ATP at 10 or 100 μmol/L and 50 μL of 5-DK-Sepharose 4B or 50 μL of Sepharose 4B (as a negative control) in reaction buffer to give a final volume of 500 μL. The mixtures were incubated at 4°C overnight with shaking. After washing, the pulled-down proteins were detected by Western blotting. Lane 2, negative control (Src, PI3K, or RSK2 does not bind Sepharose 4B); lane 3, positive control (Src, PI3K, or RSK2 binds to 5-DK-Sepharose 4B); lanes 4 and 5, increasing amounts of ATP alter the binding of 5-DK with Src, PI3K, or RSK2. Each experiment was done three times.

5-DK represses Src, PI3K, and RSK2 activities

We also investigated the effects of 5-DK on Src, PI3K, and MAPK kinase activities. The results of a kinase assay showed that 5-DK strongly inhibited Src or PI3K activity (Fig. 2A, top and middle). 5-DK was reported to be an inhibitor of RSK2 (16), and in the present study, 5-DK also dramatically attenuated RSK2 activity (Fig. 2A, bottom). To confirm the specific inhibition of Src, PI3K, and RSK2 by 5-DK, we examined the activities of other kinases; however, 5-DK had no effect on ERK, p38, or JNK kinase activity (Fig. 2B). These results imply that the inhibition of COX-2 and VEGF expression by 5-DK is mainly due to the suppression of Src, PI3K, and RSK2 activities.

5-DK specifically binds to and competes with ATP for binding to Src, PI3K, and RSK2

To confirm that the inhibition of Src, PI3K, and RSK2 activities by 5-DK is caused by a direct interaction, we performed pull-down assays using 5-DK with Src, PI3K, or RSK2. Src, PI3K, or RSK2 was pulled down by 5-DK-Sepharose 4B, but not by Sepharose 4B alone (Fig. 2C). Furthermore, the binding abilities of 5-DK to Src, PI3K, and RSK2 were decreased in the presence of ATP (Fig. 2D), indicating that 5-DK competes with ATP for binding to these protein molecules. These results suggest that 5-DK interacts with Src, PI3K, or RSK2 in an ATP-competitive manner.

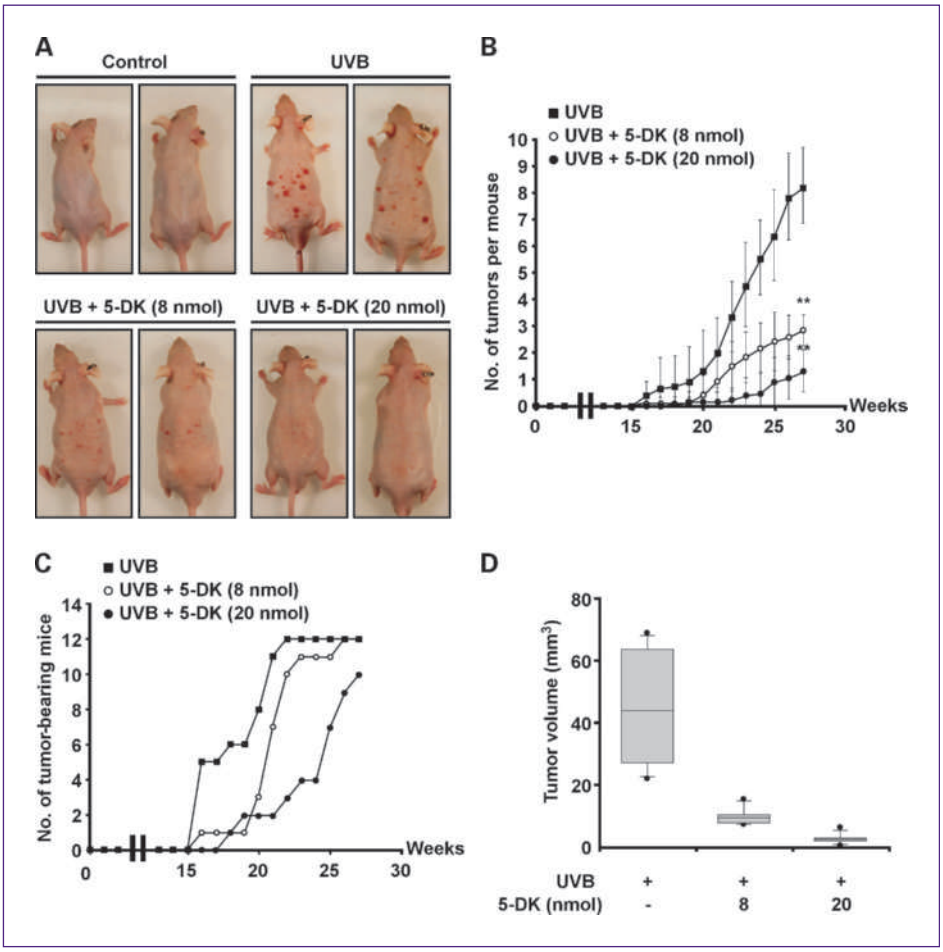

Fig. 3. Effect of 5-DK on UVB-induced skin carcinogenesis in SKH-1 hairless mice. A, external appearance of UVB-induced tumors. B, 5-DK strongly inhibits UVB-induced tumor incidence in SKH-1 hairless mice. The 12 mice in the control group received topical treatment with 200 μL of acetone; in the UVB group, the mice were treated topically with 200 μL of acetone before UVB (0.18 J/cm^2) exposure for 27 wk. The mice in the 3rd and 4th groups received topical treatment with 5-DK (8 or 20 nmol, respectively) 1 h before UVB (0.18 J/cm^2) irradiation for 27 wk. The frequency of irradiation was set at three times a week. The respective doses of 5-DK (8 or 20 nmol in 200 μL of acetone per mouse) and UVB (0.18 J/cm^2) were applied topically to the dorsal area. The incidence of skin tumors was recorded weekly. A tumor was defined as an outgrowth >1 mm in diameter that persisted for 2 wk or longer. Tumor incidence and multiplicity were recorded each week until the end of the experiment at 27 wk. C, 5-DK reduces the number of UVB-induced tumor–bearing mice. The mice were treated as described in the legend to Fig. 5B. D, 5-DK strongly inhibits UVB-induced tumor volume in mice. The mice were treated as described in the legend to Fig. 5B. At the end of the study, the dimension of each tumor in each mouse was recorded. Tumor volume was calculated using the hemiellipsoid model formula: tumor volume = 1/2 (4π/3) (*l*/2) (*w*/2) *h*, where *l* is the length, *w* is the width, and *h* is the height. The data were analyzed using the SAS software (SAS Institute) program.

5-DK suppresses UVB-induced skin tumorigenesis in SKH-1 hairless mice

To examine further the anticancer effect of 5-DK *in vivo*, we evaluated the effect of 5-DK on UVB-induced tumorigenesis in mouse skin. Topically applied 5-DK strongly inhibited UVB-induced mouse skin tumor formation compared with exposure to UVB alone (Fig. 3A). The UVB-only group averaged 8.2 tumors per mouse, whereas the 5-DK group averaged 2.8 or 1.3 tumors per mouse after treatment with 5-DK at 8 or 20 nmol, respectively (Fig. 3B). Exposure to UVB resulted in the development of skin tumors in all of the mice in the UVB-only group within 22 weeks; however, 26 weeks was required for all of the mice in the 8 nmol 5-DK group to develop tumors, and only 83% of the mice in the 20 nmol 5-DK–treated group developed

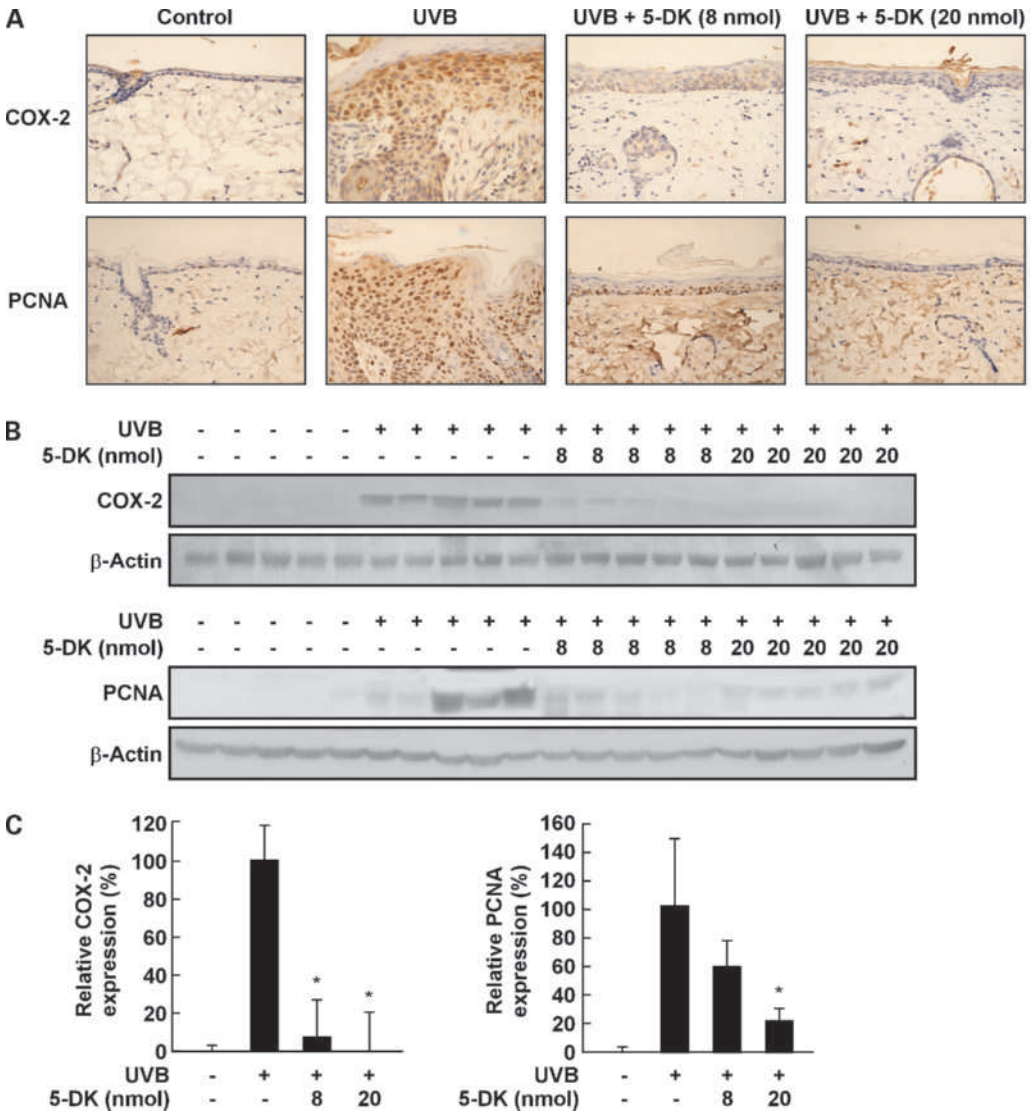

Fig. 4. Effects of 5-DK on UVB-induced COX-2 and PCNA expression in SKH-1 hairless mice. A, 5-DK inhibits UVB-induced COX-2 and PCNA expression in SKH-1 hairless mice. The mice were treated as described in the legend to Fig. 3B. Serial sections were mounted on silane-coated slides and immunostained with antibodies to detect COX-2 and PCNA, as described in Materials and Methods. The representative pictures are from five or six tissue samples. COX-2 and PCNA appear brown. B and C, 5-DK inhibits UVB-induced COX-2 and PCNA expression in SKH-1 hairless mice. The expression patterns of COX-2, PCNA, and β-actin were analyzed by Western blotting, as described in Materials and Methods, using antibodies against the corresponding proteins. All tissues or proteins were isolated from the chronic UVB carcinogenesis experiment at the end of 27 wk. Each band was densitometrically quantified by image analysis and the results were averaged ($n = 5$ each group) and are shown as means ± SD in C. *, $P < 0.05$, significant decrease in expression for the group irradiated with UVB and treated with 5-DK versus the group exposed to UVB alone.

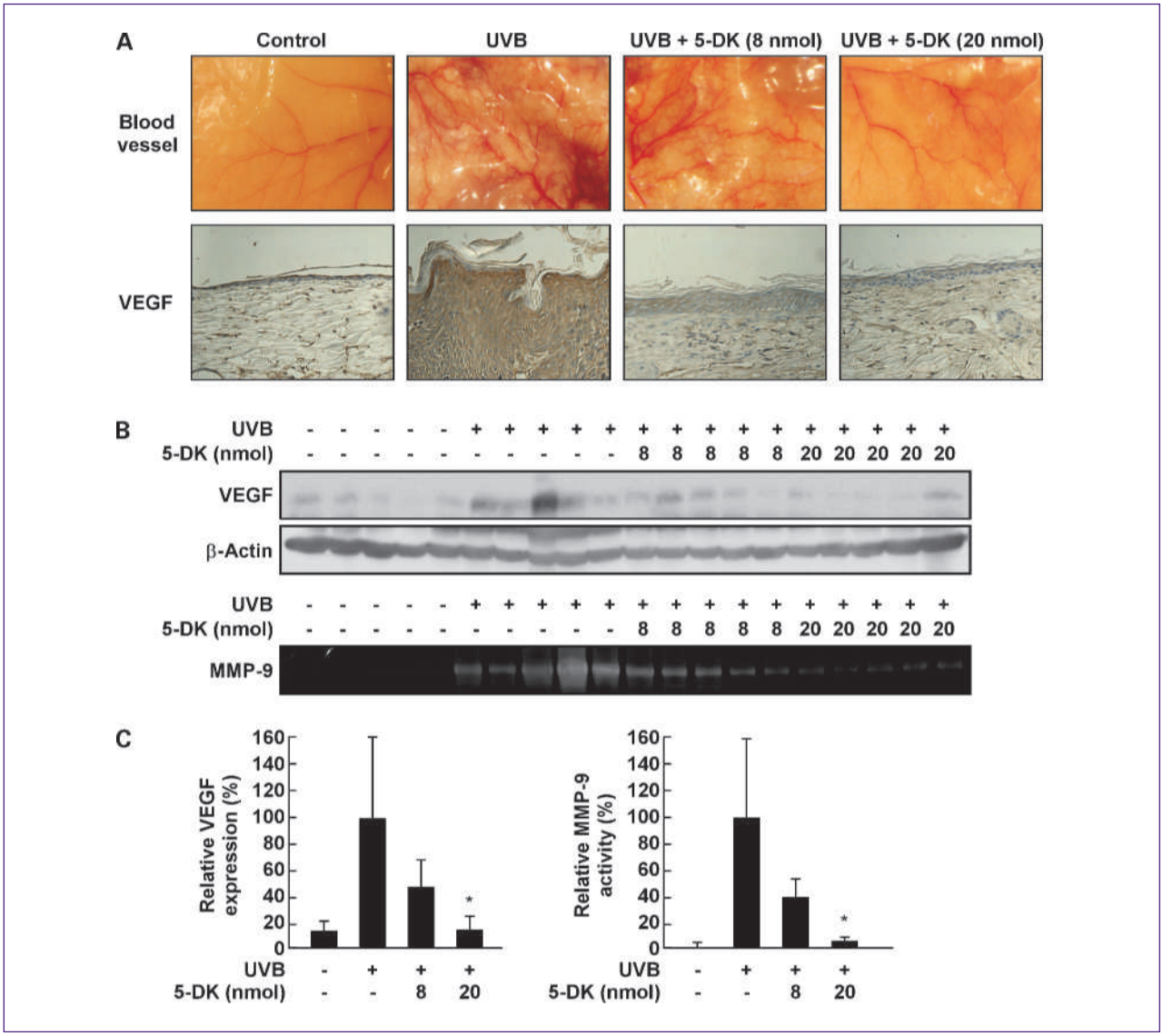

Fig. 5. Effects of 5-DK on UVB-induced blood vessel formation, VEGF expression, and MMP-9 activity in SKH-1 hairless mice. A, 5-DK inhibits UVB-induced blood vessel formation and VEGF expression in SKH-1 hairless mice. The mice were treated as described in the legend to Fig. 3B. Photographs of blood vessels were taken using a Samsung digital camera after euthanization of the animal at the end of the experiment. Serial sections were mounted on silane-coated slides and immunostained using anti-VEGF, as described in Materials and Methods. Representative pictures are from five or six tissue samples. The VEGF is stained brown. B and C, 5-DK inhibits UVB-induced VEGF expression and MMP-9 activity in SKH-1 hairless mice. The levels of VEGF and β-actin were determined by Western blotting, as described in Materials and Methods, using antibodies against the corresponding proteins. MMP-9 activity was measured by gelatin zymography, as described in Materials and Methods. All tissues or proteins were isolated from the chronic UVB carcinogenesis experiment at the end of 27 wk. Each band was densitometrically quantified by image analysis and averaged (n = 5 per group) and the results are shown as means ± SD in C. *, $P < 0.05$, significant decrease in expression for the group irradiated with UVB and treated with 5-DK versus the group exposed to UVB alone.

tumors by the end of the experiment at 27 weeks (Fig. 3C). The average tumor volume per mouse was also decreased from 86.6 mm^3 in the UVB-treated group to 19.0 mm^3 or 5.3 mm^3 in the 8 nmol or 20 nmol 5-DK–treated groups, respectively, corresponding to an 88% to 94% decrease (Fig. 3D). Overall, these results clearly show that 5-DK exerts a strong protective effect against UVB-induced tumorigenesis in mouse skin.

5-DK inhibits UVB-induced COX-2 and PCNA expression in SKH-1 hairless mice

We next assessed the effect of 5-DK on UVB-induced COX-2 expression in SKH-1 hairless mouse skin. Immunohistochemical analysis revealed that 5-DK inhibited UVB-induced COX-2 expression in the mouse skin epidermis (Fig. 4A, top). Skin tissues from mice treated with 5-DK showed strong inhibitory effects against hyperproliferation (Fig. 4A), and because enhanced proliferation is a hallmark

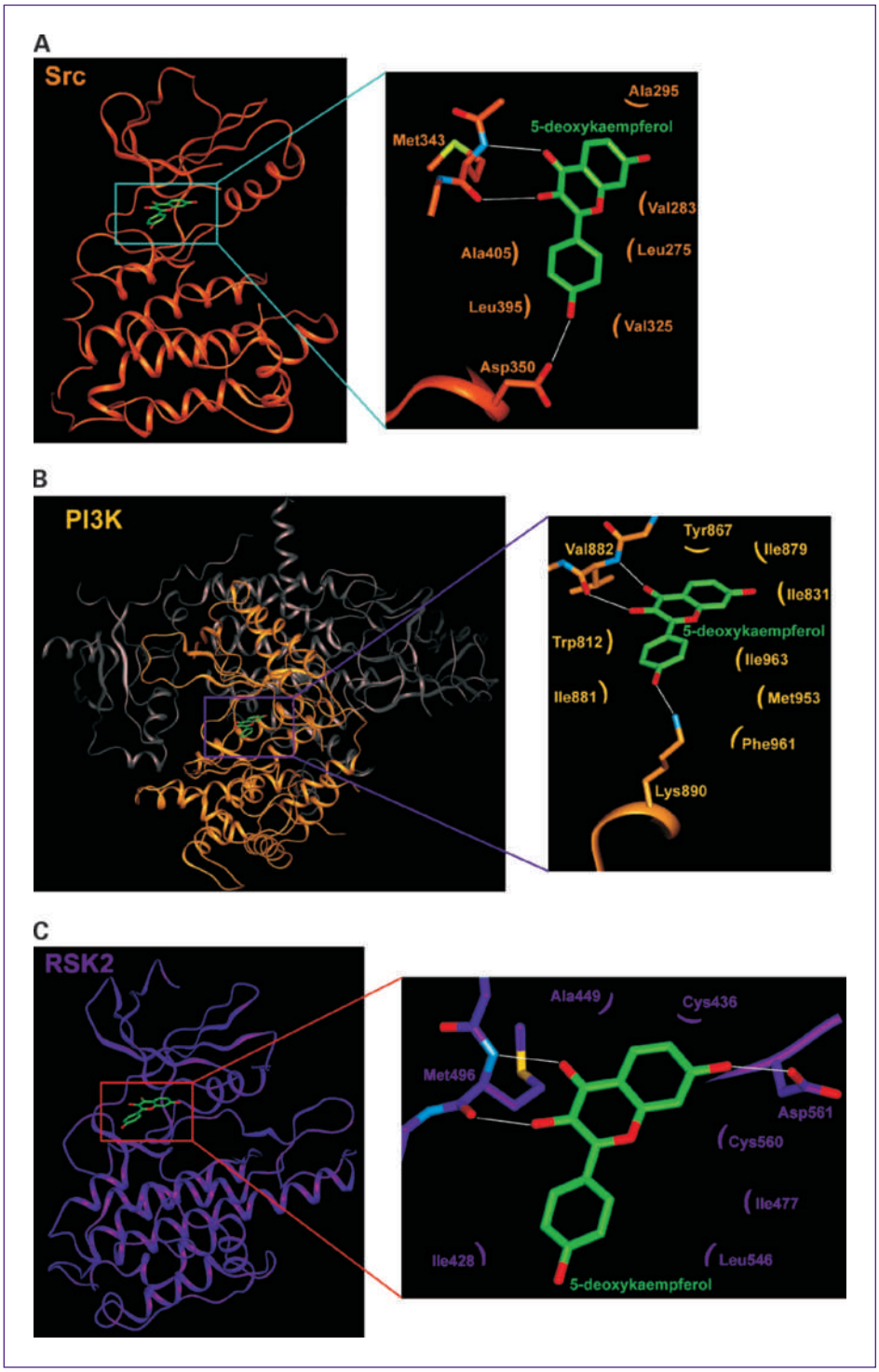

Fig. 6. Hypothetical models for kinase complexing with 5-DK. A, predicted binding mode of 5-DK to the kinase domain of Src. The hydrogen bonds are depicted as white lines, whereas the hydrophobic contacts are indicated by small curves. B, predicted binding mode of 5-DK to PI3K. The kinase domain is colored yellow, whereas the other domains are shown in gray. C, predicted binding mode of 5-DK to the kinase domain of RSK2.

of cancer (17), we evaluated the effect of 5-DK on proliferation by examining the level of PCNA. UVB-induced PCNA expression was attenuated by the topical application of 5-DK (Fig. 4A, bottom). Western blotting confirmed that 5-DK inhibited UVB-induced COX-2 and PCNA expression (Fig. 4B and C). These results indicate that UVB-induced inflammation and hyperproliferation are suppressed by 5-DK.

5-DK attenuates UVB-induced neovascularization, VEGF expression, and MMP-9 expression in SKH-1 hairless mice

To explore further the effects of 5-DK on UVB-induced skin cancer, we examined the consequences of 5-DK on angiogenic markers in UVB-exposed mouse skin treated or not treated with 5-DK. We found that 5-DK significantly

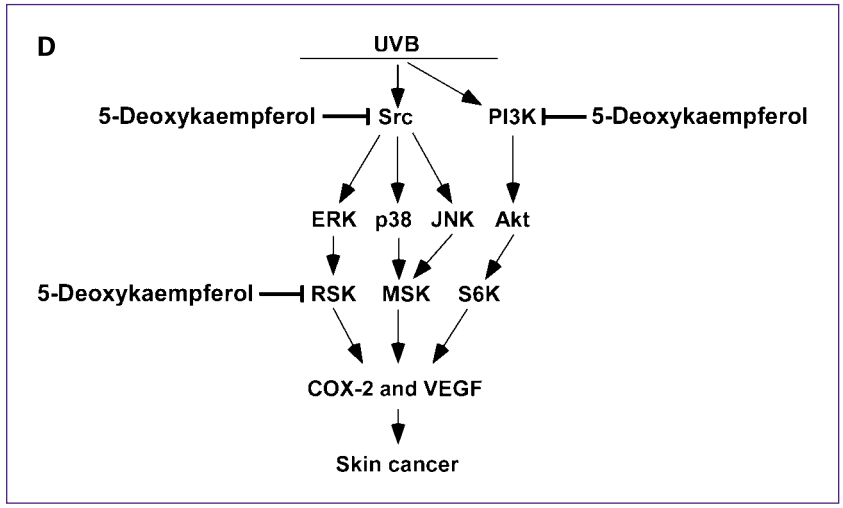

Fig. 6 *Continued.* D, simplified depiction of the proposed anti–skin cancer mechanism of 5-DK.

reduced UVB-induced blood vessel formation in mouse skin (Fig. 5A, top). In addition, 5-DK reduced epidermal VEGF expression, which was detected by immunohistochemistry (Fig. 5A, bottom). Western blot analysis confirmed that 5-DK at 8 or 20 nmol inhibited UVB-induced VEGF expression by 50% or 81%, respectively (Fig. 5B and C). Extracellular matrix remodeling through MMP upregulation is essential for irregular new blood vessel formation. Therefore, we also examined the effect of 5-DK on UVB-induced MMP-9 activity. Topical administration of 5-DK at 8 or 20 nmol suppressed UVB-induced MMP-9 activity by 88% or 97%, respectively (Fig. 5B and C). Overall, our results indicate that 5-DK exerts protective effects against UVB-induced angiogenesis and skin cancer in mouse skin.

Discussion

Flavonoids are considered to exert chemopreventive effects on the development of various cancers (18, 19). However, the cancer-chemopreventive effect of the flavonoid 5-DK has not been reported. In the present study, we show for the first time that 5-DK has strong chemopreventive effects on UVB-mediated skin carcinogenesis. Treatment with 5-DK decreased the expression of COX-2 and VEGF in JB6 P+ cells, which may explain its strong chemopreventive effect. Several studies have shown that COX-2 and VEGF are critical for UVB-induced skin carcinogenesis. Many groups have reported aberrant COX-2 expression in various human cancers, including skin cancer (20, 21), and a specific inhibitor of COX-2 was shown to prevent UVB-induced carcinomas in murine skin (22, 23). The upregulation of VEGF is an important factor in tumor vascularization and a key regulator of angiogenesis in skin inflammation (24). Therefore, our current findings suggest the usefulness of 5-DK in the prevention of skin cancer.

The anti-inflammatory and antiangiogenic effects of 5-DK may be attributed to the inhibition of UVB-induced active mitogenic and cell survival signaling in skin cancer. Previous studies indicated that the MAPK and PI3K/Akt pathways are involved in UVB-induced COX-2 and VEGF expression (25–27). Therefore, we investigated whether the inhibition of MAPK phosphorylation by 5-DK could suppress UVB-stimulated COX-2 and VEGF expression. Our results indicate that 5-DK inhibits UVB-induced phosphorylation of p38, JNK, and Akt. Because 5-DK suppressed the activation of MAPK kinase signaling and Akt, but not ERK, we hypothesize that the molecular targets of 5-DK are the upstream kinases of MAPK kinases and Akt and a downstream kinase of ERK. We expected that phosphorylation of ERKs would decrease because of inhibition of Src activity by 5-DK. However, phosphorylation of ERKs was sustained. Some have reported that under some conditions, cross talk between PI3K/Akt and MEK/ERK signaling could occur (28). Because 5-DK inhibits not only Src but also PI3K, suppression of the PI3K/Akt pathway might have increased phosphorylation of ERKs. Src is a clinically relevant oncogenic kinase that has been implicated in the progression of many types of cancer (7). The Src signaling pathway is now considered to be as important as the MAPK pathway for cell survival and proliferation (29). PI3K/Akt signaling plays a major role in several processes associated with skin tumorigenesis (30). RSK, which is a downstream substrate of ERKs, is a key regulator of tumor promoter–induced cell transformation (16).

Therefore, the identification of inhibitors of Src, PI3K, and RSK activities offers a novel therapeutic strategy. We found that treatment with 5-DK strongly inhibited Src, PI3K, and RSK2 activities, but not ERK, p38, or JNK activities, suggesting that 5-DK acts as a multikinase inhibitor of Src, PI3K, and RSK2. The most important limiting factor in target-based therapy is the narrow target specificity of the agents used, which may be overcome by targeting alternative kinase pathways that are also hyperactivated during cancer progression. Therefore, the use of multitarget chemopreventive agents may be a useful tool for avoiding these limitations (13, 14).

To investigate the molecular mechanism underlying 5-DK inhibition of Src, PI3K, and RSK, we carried out a

modeling study using the crystal structures of the respective kinases (31–33). The catalytic domains of the kinases consist of an N-lobe and a C-lobe with similar folding, and this structural similarity extends to the ATP-binding site flanked by the two lobes. The N- and C-lobes are linked by a loop, which is known as the hinge region. The backbone of the loop interacts with the adenine moiety of ATP through hydrogen bonds. Considering the finding that 5-DK is an ATP-competitive inhibitor of Src, PI3K, and RSK2, we docked this compound in the ATP-binding site of each kinase (Fig. 6A-C). Interestingly, our results suggest that 5-DK interacts with the backbone of the hinge region in each kinase in a similar manner. The hydroxyl group at position 3 and the carbonyl group at position 4 in the compound form two hydrogen bonds with Met343, Val882, and Met496 in Src, PI3K, and RSK2, respectively. The hydroxyl group at position 4′ in 5-DK can form an additional hydrogen bond with Asp350 of Src and Lys890 of PI3K. In RSK2, an additional hydrogen bond may be formed by the interaction of Asp561 with the hydroxyl group at position 7 instead of 4′. In addition, the inhibitor may be sandwiched by the side chains of the hydrophobic residues in the ATP-binding sites of the kinases, which include Ala295, Ala405, Leu395, Val325, Leu275, and Val283 of Src; Tyr867, Trp812, Ile881, Phe961, Met953, Ile963, Ile831, and Ile879 of PI3K; and Ala449, Ile428, Leu546, Lle477, Cys560, and Cys436 of RSK2. 5-DK binds in the ATP pocket of Src, PI3K, and RSK, and thus this may explain why 5-DK does not affect the phosphorylation level of the target kinases but merely affects the activity of target kinases to phosphorylate downstream molecules of Src, PI3K, and RSK. Additional X-ray crystallographic studies to determine the inhibitor-complex structures may elucidate the exact binding modes of 5-DK to Src, PI3K, and RSK2.

To examine the novel effects of 5-DK on UVB-induced skin cancer *in vivo*, we used a multistage mouse skin carcinogenesis model. Topical application of 5-DK strongly inhibited skin tumor development in SKH-1 hairless mice by decreasing the number and volume of the tumors and also by delaying tumor initiation. Specifically, UVB enhanced COX-2 and PCNA expression, promoted vascular formation and VEGF expression, and increased MMP-9 activity. Moreover, these events were strongly suppressed by topical 5-DK treatment, leading to significant photoprotection. The *in vivo* antitumor effect of 5-DK was observed in conjunction with its anti-inflammatory, antiproliferative, and antiangiogenic activities. The effects of 5-DK were accompanied by decreases in COX-2 and VEGF expression in JB6 P+ cells. A simplified depiction of our proposed mechanism for the anti–skin tumor effects of 5-DK is shown in Fig. 6D. Thus, our data support the hypothesis that natural products, such as 5-DK, can have functional effects on skin cancer both *in vitro* and *in vivo* by selectively inhibiting Src, PI3K, and RSK2 activities. 5-DK represents a natural compound that should be considered as a multimolecule-targeting inhibitor for the clinical prevention or treatment of skin cancer.

Disclosure of Potential Conflicts of Interest

No potential conflicts of interest were disclosed.

Grant Support

The Hormel Foundation; NIH grants CA27502, CA120388, CA111536, CA88961, and CA81064; BioGreen21 Program grants 20070301-034-027 and 20070301-034-042; Rural Development Administration and World Class University Program grant R31-2008-00-10056-0; Priority Research Centers Program grant 2009-0093824; the National Research Foundation of Korea; and the Ministry of Education, Science, and Technology, Republic of Korea.

The costs of publication of this article were defrayed in part by the payment of page charges. This article must therefore be hereby marked *advertisement* in accordance with 18 U.S.C. Section 1734 solely to indicate this fact.

Received 06/29/2009; revised 10/26/2009; accepted 11/06/2009; published OnlineFirst 03/16/2010.

References

1. Katiyar SK, Korman NJ, Mukhtar H, Agarwal R. Protective effects of silymarin against photocarcinogenesis in a mouse skin model. J Natl Cancer Inst 1997;89:556–66.
2. Afaq F, Adhami VM, Mukhtar H. Photochemoprevention of ultraviolet B signaling and photocarcinogenesis. Mutat Res 2005;571:153–73.
3. Aubin F, Humbey O, Humbert P, Laurent R, Mougin C. [Melanoma: role of ultraviolet radiation: from physiology to pathology]. Presse Med 2001;30:546–51.
4. Surh YJ, Kundu JK. Cancer preventive phytochemicals as speed breakers in inflammatory signaling involved in aberrant COX-2 expression. Curr Cancer Drug Targets 2007;7:447–58.
5. Roy S, Khanna S, Alessio HM, et al. Anti-angiogenic property of edible berries. Free Radic Res 2002;36:1023–31.
6. Melnikova VO, Ananthaswamy HN. Cellular and molecular events leading to the development of skin cancer. Mutat Res 2005;571:91–106.
7. Irby RB, Yeatman TJ. Role of Src expression and activation in human cancer. Oncogene 2000;19:5636–42.
8. Rahimi N, Hung W, Tremblay E, Saulnier R, Elliott B. c-Src kinase activity is required for hepatocyte growth factor-induced motility and anchorage-independent growth of mammary carcinoma cells. J Biol Chem 1998;273:33714–21.
9. Summy JM, Gallick GE. Src family kinases in tumor progression and metastasis. Cancer Metastasis Rev 2003;22:337–58.
10. Thomas SM, Brugge JS. Cellular functions regulated by Src family kinases. Annu Rev Cell Dev Biol 1997;13:513–609.
11. Fecker LF, Stockfleth E, Nindl I, Ulrich C, Forschner T, Eberle J. The role of apoptosis in therapy and prophylaxis of epithelial tumours by nonsteroidal anti-inflammatory drugs (NSAIDs). Br J Dermatol 2007;156 Suppl 3:25–33.
12. Rak J, Yu JL, Klement G, Kerbel RS. Oncogenes and angiogenesis: signaling three-dimensional tumor growth. J Investig Dermatol Symp Proc 2000;5:24–33.
13. Imai K, Takaoka A. Comparing antibody and small-molecule therapies for cancer. Nat Rev Cancer 2006;6:714–27.
14. Vogt PK, Kang S. Kinase inhibitors: vice becomes virtue. Cancer Cell 2006;9:327–8.
15. Gonnet JF, Jay M. Les aglycones flavoniques d'*Anthyllis vulneraria*. Phytochemistry 1972;11:2313–6.
16. Cho YY, Yao K, Kim HG, et al. Ribosomal S6 kinase 2 is a key

regulator in tumor promoter induced cell transformation. Cancer Res 2007;67:8104–12.
17. Hanahan D, Weinberg RA. The hallmarks of cancer. Cell 2000;100: 57–70.
18. Surh YJ. Cancer chemoprevention with dietary phytochemicals. Nat Rev Cancer 2003;3:768–80.
19. Yang CS, Lee MJ, Chen L, Yang GY. Polyphenols as inhibitors of carcinogenesis. Environ Health Perspect 1997;105 Suppl 4:971–6.
20. Buckman SY, Gresham A, Hale P, et al. COX-2 expression is induced by UVB exposure in human skin: implications for the development of skin cancer. Carcinogenesis 1998;19:723–9.
21. Denkert C, Kobel M, Berger S, et al. Expression of cyclooxygenase 2 in human malignant melanoma. Cancer Res 2001;61:303–8.
22. Pentland AP, Schoggins JW, Scott GA, Khan KN, Han R. Reduction of UV-induced skin tumors in hairless mice by selective COX-2 inhibition. Carcinogenesis 1999;20:1939–44.
23. Tang X, Kim AL, Kopelovich L, Bickers DR, Athar M. Cyclooxygenase-2 inhibitor nimesulide blocks ultraviolet B-induced photocarcinogenesis in SKH-1 hairless mice. Photochem Photobiol 2008;84: 522–7.
24. Larcher F, Robles AI, Duran H, et al. Up-regulation of vascular endothelial growth factor/vascular permeability factor in mouse skin carcinogenesis correlates with malignant progression state and activated H-ras expression levels. Cancer Res 1996;56: 5391–6.
25. Bachelor MA, Bowden GT. UVA-mediated activation of signaling pathways involved in skin tumor promotion and progression. Semin Cancer Biol 2004;14:131–8.
26. Bode AM, Dong Z. Mitogen-activated protein kinase activation in UV-induced signal transduction. Sci STKE 2003;2003:RE2.
27. Li Y, Bi Z, Yan B, Wan Y. UVB radiation induces expression of HIF-1α and VEGF through the EGFR/PI3K/DEC1 pathway. Int J Mol Med 2006;18:713–9.
28. Dai R, Chen R, Li H. Cross-talk between PI3K/Akt and MEK/ERK pathways mediates endoplasmic reticulum stress-induced cell cycle progression and cell death in human hepatocellular carcinoma cells. Int J Oncol 2009;34:1749–57.
29. Devary Y, Gottlieb RA, Smeal T, Karin M. The mammalian ultraviolet response is triggered by activation of Src tyrosine kinases. Cell 1992; 71:1081–91.
30. Bachelor MA, Cooper SJ, Sikorski ET, Bowden GT. Inhibition of p38 mitogen-activated protein kinase and phosphatidylinositol 3-kinase decreases UVB-induced activator protein-1 and cyclooxygenase-2 in a SKH-1 hairless mouse model. Mol Cancer Res 2005;3:90–9.
31. Breitenlechner CB, Kairies NA, Honold K, et al. Crystal structures of active SRC kinase domain complexes. J Mol Biol 2005;353:222–31.
32. Malakhova M, Tereshko V, Lee SY, et al. Structural basis for activation of the autoinhibitory C-terminal kinase domain of p90 RSK2. Nat Struct Mol Biol 2008;15:112–3.
33. Walker EH, Pacold ME, Perisic O, et al. Structural determinants of phosphoinositide 3-kinase inhibition by wortmannin, LY294002, quercetin, myricetin, and staurosporine. Mol Cell 2000;6:909–19.